

Contents

*c1ccc(cc1)C2CN(CS2)C(=O)N[R2]

Figure 1 is a line graph showing the tumor volume (mm³) over time (Days after tumor cell inoculation) for four groups: Control, Compound 1b 5mg/kg, DTIC 60mg/kg, and Compound 1b 10mg/kg. The y-axis represents Tumor Volume (mm³) ranging from 0 to 2500. The x-axis represents Days after tumor cell inoculation ranging from 5 to 35. A vertical line at day 7 indicates the start of treatment. The Control group shows the highest tumor growth, reaching approximately 2000 mm³ by day 35. The Compound 1b 10mg/kg group shows the lowest tumor growth, reaching approximately 800 mm³ by day 35. The DTIC 60mg/kg group shows intermediate growth, reaching approximately 1200 mm³ by day 35. The Compound 1b 5mg/kg group shows growth similar to the DTIC group, reaching approximately 1500 mm³ by day 35. Error bars represent standard deviation.

Days after tumor cell inoculation	Control (mm³)	Compound 1b 5mg/kg (mm³)	DTIC 60mg/kg (mm³)	Compound 1b 10mg/kg (mm³)
5	~150	~150	~150	~150
7	~150	~150	~150	~150
10	~150	~150	~150	~150
12	~200	~150	~150	~150
15	~300	~250	~250	~150
18	~450	~350	~350	~200
22	~700	~600	~550	~400
25	~1100	~1000	~700	~550
28	~1300	~1100	~850	~550
30	~1600	~1250	~1050	~700
35	~2000	~1500	~1200	~800



Reaction scheme showing the synthesis of compound 5 from Malaisia ericifolia. The starting material is a substituted phenol derivative (with a vinyl group and a methoxy group) and an aryl boronic acid (Ar(BOH)₂). The reaction conditions are: Et₃N, Pd(OAc)₂, PPh₃, CH₂Cl₂, 80 °C, N₂, 3 h. The reaction yields two products: Product (E2) and the Major product (E). The structure of Malaisia ericifolia is shown as a photograph. The chemical structure of the major product (E) is shown with a 3D ball-and-stick model and a 2D chemical structure.



Chemical reaction scheme showing the synthesis of a nucleoside derivative. The starting material is a nucleoside with a 4-chlorobenzyl group and a terminal alkyne. It reacts with a reporter group Y to form a nucleoside with the reporter group attached via a triazole ring. The nucleoside part is a ribose derivative with a 4-chlorobenzyl group and a terminal alkyne. The reaction is catalyzed by CuI and CuBr, with NaHCO₃ and Na₂CO₃ as bases, in DMF at 100°C for 24 hours. The product is a nucleoside with the reporter group Y attached via a triazole ring. Y is defined as a reporter group, bioactive molecule, or carrier.

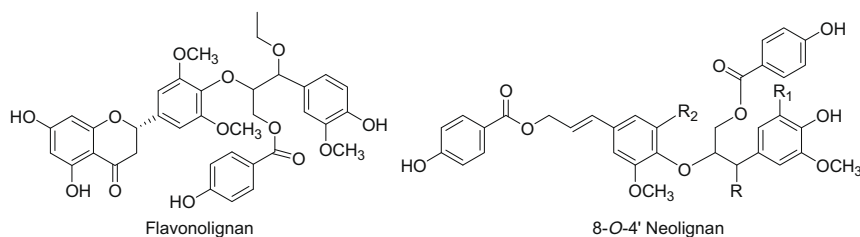
Y = reporter group, bioactive molecule, or carrier



Quiquelignan A–H, eight new lignoids from the rattan palm *Calamus quiquesetinervius* and their antiradical, anti-inflammatory and antiplatelet aggregation activities

pp 518–525

Chao-Lin Chang, Li-Jie Zhang, Ru-Yin Chen, Chin-Chung Wu, Hui-Chi Huang, Michael C. Roy, Jhih-Ping Huang, Yang-Chang Wu^{*}, Yao-Haur Kuo^{*}

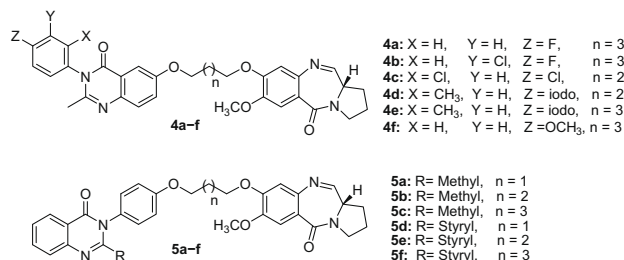


Three new flavonlignans (**1–3**) and five new 8-O-4' neolignan derivatives (**4–8**) were isolated from the EtOAc extract of *Calamus quiquesetinervius*.

Quinazolinone linked pyrrolo[2,1-c][1,4]benzodiazepine (PBD) conjugates: Design, synthesis and biological evaluation as potential anticancer agents

pp 526–542

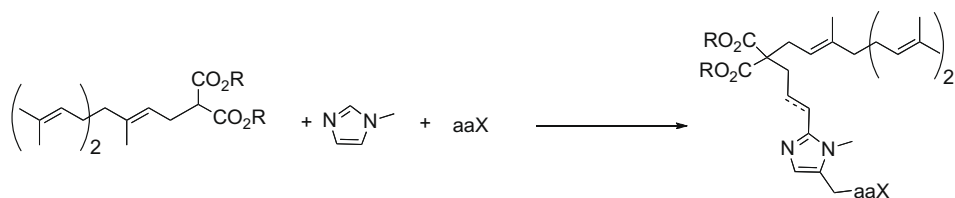
Ahmed Kamal^{*}, E. Vijaya Bharathi, M. Janaki Ramaiah, D. Dastagiri, J. Surendranadha Reddy, A. Viswanath, Farheen Sultana, S. N. C. V. L. Pushpavalli, Manika Pal-Bhadra^{*}, Hemant Kumar Srivastava, G. Narahari Sastry^{*}, Aarti Juvekar, Subrata Sen, Surekha Zingde



Towards the synthesis of bisubstrate inhibitors of protein farnesyltransferase: Synthesis and biological evaluation of new farnesylpyrophosphate analogues

pp 543–556

Stéphanie Duez, Laëtizia Coudray, Elisabeth Mouray, Philippe Grellier, Joëlle Dubois^{*}



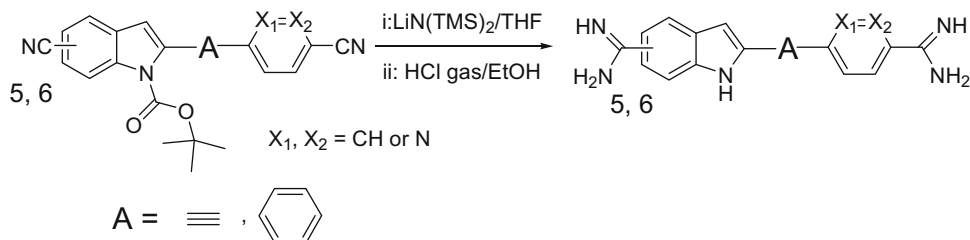
New FPP analogues were synthesized. The most active derivative was coupled to aaX motif through the imidazole ring affording new FTase inhibitors active against *Plasmodium falciparum* and *Trypanosoma brucei*.



Synthesis, DNA binding, fluorescence measurements and antiparasitic activity of DAPI related diamidines

pp 557–566

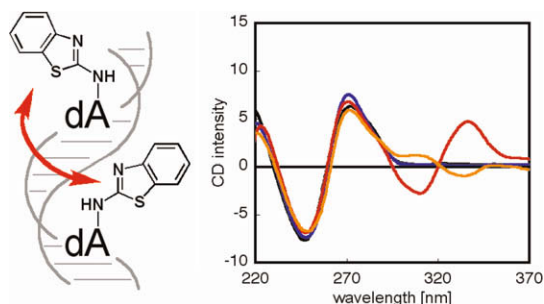
Abdelbasset A. Farahat, Arvind Kumar, Martial Say, Alaa El-Din M. Barghash, Fatma E. Goda, Hassan M. Eisa, Tanja Wenzler, Reto Brun, Yang Liu, Leah Mickelson, W. David Wilson, David W. Boykin^{*}



Synthesis of 6-*N*-(benzothiazol-2-yl)deoxyadenosine and its exciton-coupled circular dichroism

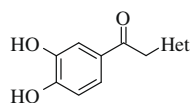
pp 567–572

Yoshiaki Masaki, Akihiro Ohkubo, Kohji Seio, Mitsuo Sekine *

**Design and synthesis of selective inhibitors of Placental Alkaline Phosphatase**

pp 573–579

Marion Lanier *, Eduard Sergienko, Ana Maria Simão, Ying Su, Thomas Chung, José Luis Millán, John R. Cashman

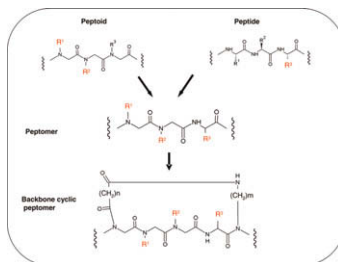


A series of catechols was selected and evaluated as selective inhibitors of PLAP over the other AP isozymes. SAR is reported.

The effect of backbone cyclization on PK/PD properties of bioactive peptide-peptoid hybrids: The melanocortin agonist paradigm

pp 580–589

Oded Ovadia, Yaniv Linde, Carrie Haskell-Luevano, Marvin L. Dirain, Tanya Sheynis, Raz Jelinek, Chaim Gilon, Amnon Hoffman *

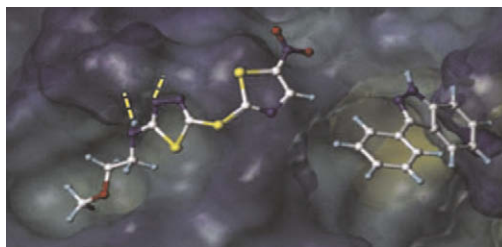


General structure of peptides, peptoids, peptomers and backbone cyclic peptomers.

**Synthesis and optimization of thiadiazole derivatives as a novel class of substrate competitive c-Jun N-terminal kinase inhibitors**

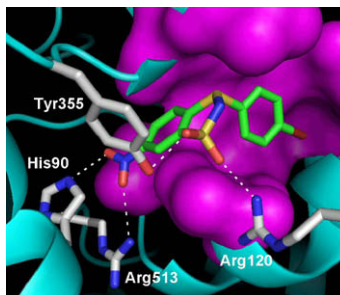
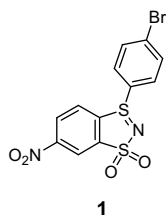
pp 590–596

Surya K. De, Vida Chen, John L. Stebbins, Li-Hsing Chen, Jason F. Cellitti, Thomas Machleidt, Elisa Barile, Megan Riel-Mehan, Russell Dahl, Li Yang, Aras Emdadi, Ria Murphy, Maurizio Pellecchia *

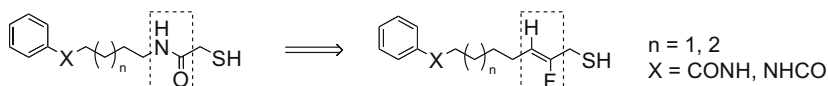


Discovery of 3-(4-bromophenyl)-6-nitrobenzo[1.3.2]dithiazolium ylide 1,1-dioxide as a novel dual cyclooxygenase/5-lipoxygenase inhibitor that also inhibits tumor necrosis factor- α production

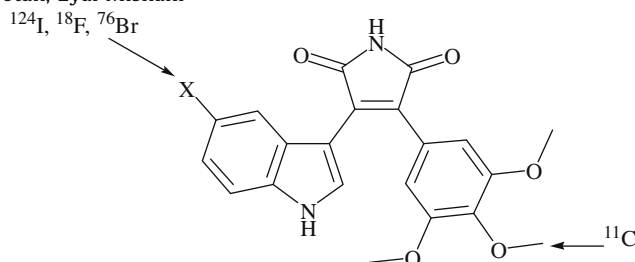
pp 597–604

 Chien-Shu Chen, Chen-Ming Tan, Chiung-Hua Huang, Ling-Chu Chang, Jih-Pyang Wang, Fong-Chi Cheng, Ji-Wang Chern^{*}

Fluoroalkene modification of mercaptoacetamide-based histone deacetylase inhibitors

pp 605–611

 Satoshi Osada^{*}, Satoshi Sano, Mariko Ueyama, Yoshiro Chuman, Hiroaki Kodama, Kazuyasu Sakaguchi

Labeled 3-aryl-4-indolylmaleimide derivatives and their potential as angiogenic PET biomarkers

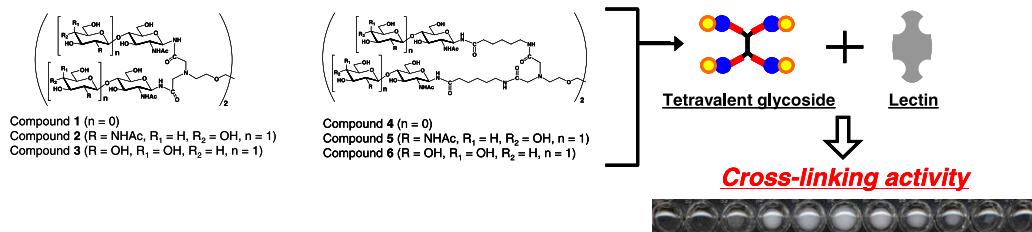
pp 612–620

 Ohad Ilovich, Hana Billauer, Sharon Dotan, Eyal Mishani^{*}

 $X = \text{H}, \text{F}, \text{Br}, \text{I}$

New 3-aryl-4-indolylmaleimide derivatives were synthesized and evaluated as potential PET biomarkers for monitoring angiogenic processes.

Molecular design of N-linked tetravalent glycosides bearing N-acetylglucosamine, N,N'-diacetylchitobiose and N-acetyllactosamine: Analysis of cross-linking activities with WGA and ECA lectins

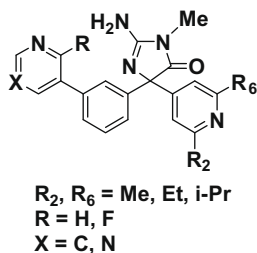
pp 621–629

 Ryuichi Masaka, Makoto Ogata, Yoshinori Misawa, Megumi Yano, Chika Hashimoto, Takeomi Murata, Hirokazu Kawagishi, Taichi Usui^{*}


Di-substituted pyridinyl aminohydantoin s as potent and highly selective human β -secretase (BACE1) inhibitors

pp 630–639

Michael S. Malamas^{*}, Keith Barnes, Matthew Johnson, Yu Hui, Ping Zhou, Jim Turner, Yun Hu, Erik Wagner, Kristi Fan, Rajiv Chopra, Andrea Olland, Jonathan Bard, Menelas Pangelos, Peter Reinhart, Albert J. Robichaud



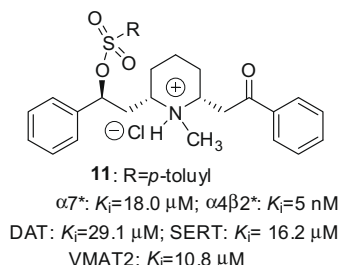
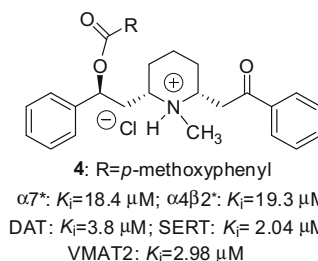
Steric substituents close to the BACE1 Pro₇₀/BACE2 Lys₈₆ mutation has generated a conflict between the ligand and the BACE2 enzyme backbone, thus resulting in highly selective BACE1 inhibitors.

Lobeline esters as novel ligands for neuronal nicotinic acetylcholine receptors and neurotransmitter transporters

pp 640–649

Marhaba Hojahmat, David B. Horton, Seth D. Norrholm, Dennis K. Miller, Vladimir P. Grinevich, Agripina Gabriela Deaciuc, Linda P. Dwoskin, Peter A. Crooks^{*}

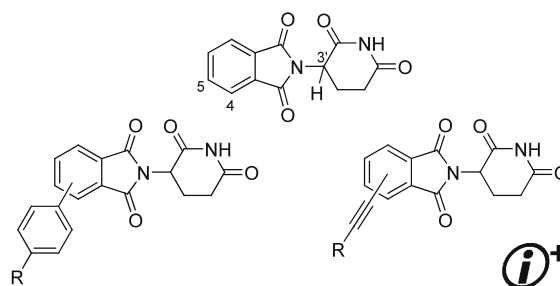
A series of carboxylate and sulfonate esters of lobeline have been synthesized. The sulfonate esters exhibited high affinity ($K_i = 5\text{--}17$ nM), at $\alpha 4\beta 2^*$ nicotinic receptors, but were less active as inhibitors of neurotransmitter transporters. The carboxylate esters had lower affinity at $\alpha 4\beta 2^*$ nicotinic receptors ($0.06\text{--}19.3$ μM) and moderate affinity and selectivity at neurotransmitter transporters.

**New thalidomide analogues derived through Sonogashira or Suzuki reactions and their TNF expression inhibition profiles**

pp 650–662

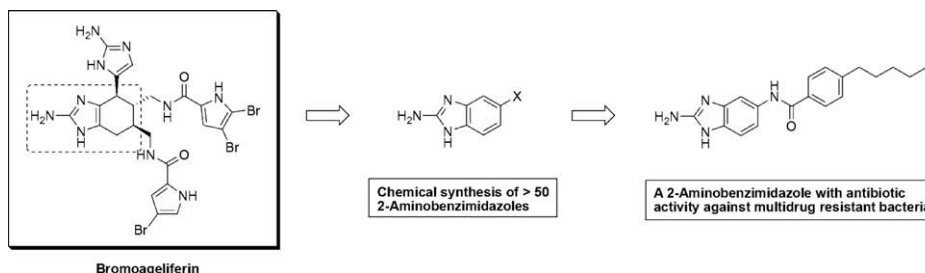
Scott G. Stewart^{*}, Carlos J. Braun, Sze-Ling Ng, Marta E. Polomska, Mahdad Karimi, Lawrence J. Abraham

Thalidomide analogues containing either a phenyl or alkyne tether were prepared using cross coupling reactions. Several analogues were far more efficient in the inhibition of the expression of the Tumour Necrosis Factor (TNF) monitored through a novel reporter system. Several derivatives showed increased cytotoxicity due to induction of an apoptotic response.

**The chemical synthesis and antibiotic activity of a diverse library of 2-aminobenzimidazole small molecules against MRSA and multidrug-resistant *A. baumannii***

pp 663–674

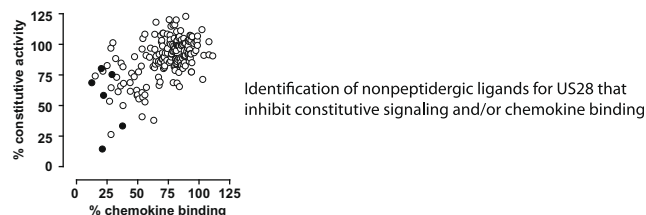
Robert W. Huigens III, Samuel Reyes, Catherine S. Reed, Cynthia Bunders, Steven A. Rogers, Andrew T. Steinhauer, Christian Melander^{*}



Identification of novel allosteric nonpeptidergic inhibitors of the human cytomegalovirus-encoded chemokine receptor US28

pp 675–688

Henry F. Vischer^{*}, Janneke W. Hulshof, Saskia Hulscher, Silvina A. Fratantoni, Mark H. P. Verheij, Jane Victorina, Martine J. Smit, Iwan J. P. de Esch, Rob Leurs

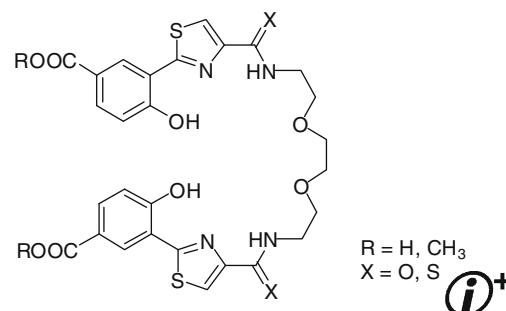


Synthesis and biological properties of iron chelators based on a bis-2-(2-hydroxy-phenyl)-thiazole-4-carboxamide or -thiocarboxamide (BHPTC) scaffold

pp 689–695

David Rodriguez-Lucena, François Gaboriau, Freddy Rivault, Isabelle J. Schalk, Gérard Lescoat, Gaëtan L. A. Mislin^{*}

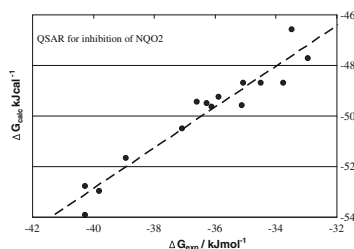
Bis-2-(2-hydroxy-phenyl)-thiazole-4-carboxamides or -thiocarboxamides (BHPTCs) are efficient bis-tridentate iron chelators with promising biological properties: lipophilic dithioamide BHPTC (R = CH₃, X = S) displayed in vitro an antiproliferative activity on several cancerous cell lines when hydrophilic diamide BHPTC (R = H, X = O) proved to be as efficient and less toxic as deferoxamine (DFO) when tested for its cytoprotective activity against iron overload.



Triazoloacridin-6-ones as novel inhibitors of the quinone oxidoreductases NQO1 and NQO2

pp 696–706

Karen A. Nolan, Matthew P. Humphries, John Barnes, Jeremy R. Doncaster, Mary C. Caraher, Nicola Tirelli, Richard A. Bryce, Roger C. Whitehead, Ian J. Stratford^{*}



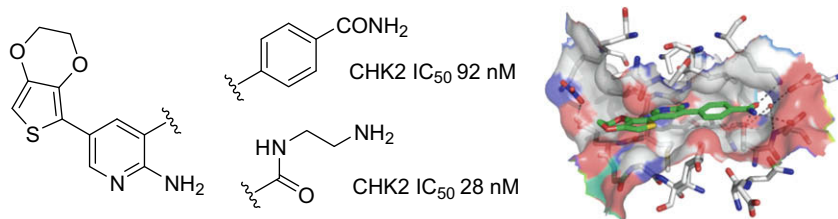
A series of 5-, 8-substituted triazoloacridin-6-ones have been synthesized and biologically evaluated as novel inhibitors of the quinone oxidoreductases, NQO1 and NQO2. Molecular modeling provides insights into their structure–activity behaviour and selectivity.



Identification and characterisation of 2-aminopyridine inhibitors of checkpoint kinase 2

pp 707–718

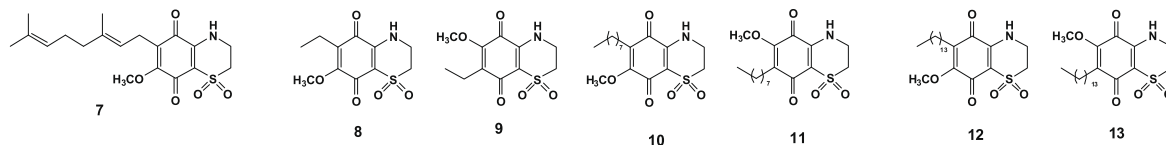
Stephen Hilton, Sebastien Naud, John J. Caldwell, Kathy Boxall, Samantha Burns, Victoria E. Anderson, Laurent Antoni, Charlotte E. Allen, Laurence H. Pearl, Antony W. Oliver, G. Wynne Aherne, Michelle D. Garrett, Ian Collins^{*}



Synthesis of structurally simplified analogues of aplidinone A, a pro-apoptotic marine thiazinoquinone

pp 719–727

Anna Aiello, Ernesto Fattorusso, Paolo Luciano, Marialuisa Menna^{*}, Marco A. Calzado, Eduardo Muñoz, Francesco Bonadies, Marcella Guiso, Maria Filomena Sanasi, Gianfranco Cocco, Rosario Nicoletti

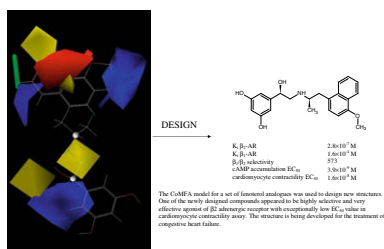


Structurally simplified analogues (**8–13**) of aplidinone A (**7**) have been synthesized. Compound **11** is a potent pro-apoptotic agent which also inhibits the TNF α -induced NF- κ B activation in human leukemia T cells.

Comparative molecular field analysis of fenoterol derivatives: A platform towards highly selective and effective β_2 -adrenergic receptor agonists

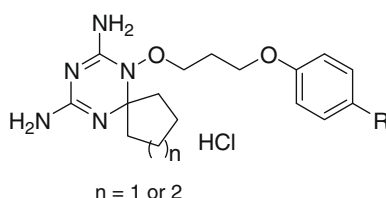
pp 728–736

Krzysztof Jozwiak^{*}, Anthony Yiu-Ho Woo, Mary J. Tanga, Lawrence Toll, Lucita Jimenez, Joseph A. Kozocas, Anita Plazinska, Rui-Ping Xiao, Irving W. Wainer

**Antifolate and antiproliferative activity of 6,8,10-triazaspiro[4.5]deca-6,8-dienes and 1,3,5-triazaspiro[5.5]undeca-1,3-dienes**

pp 737–743

Xiang Ma^{*}, Wai-Keung Chui^{*}

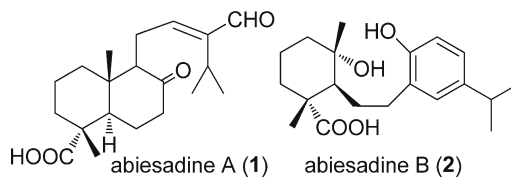


Antifolate agents with *para* substitution R on phenyl ring according to Craig plot were prepared and investigated in vitro for DHFR inhibitory activity and antiproliferative activity against A549 cancer cells.

Isolation, structure, and bioactivities of abiesadines A–Y, 25 new diterpenes from *Abies georgei* Orr

pp 744–754

Xian-Wen Yang, Lin Feng, Su-Mei Li, Xiao-Hua Liu, Yong-Li Li, Liang Wu, Yun-Heng Shen, Jun-Mian Tian, Xi Zhang, Xin-Ru Liu, Ning Wang, Yonghong Liu, Wei-Dong Zhang



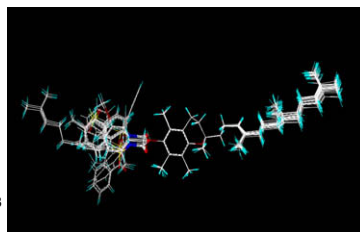
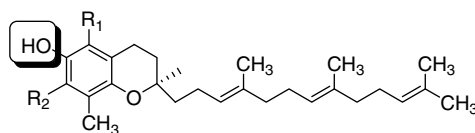
Twenty-five new diterpenes, abiesadines A–Y (**1–25**) were isolated from the aerial parts of *Abies georgei* together with 29 known ones (**26–54**).



Design and preliminary structure–activity relationship of redox-silent semisynthetic tocotrienol analogues as inhibitors for breast cancer proliferation and invasion

pp 755–768

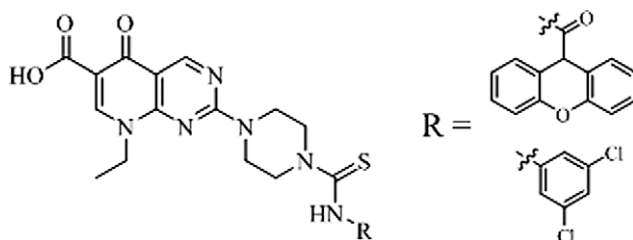
Ahmed Y. Elnagar, Vikram B. Wali, Paul W. Sylvester, Khalid A. El Sayed *



Characterization of non-lipid autotaxin inhibitors

pp 769–776

Adrienne B. Hoeglund, Angela L. Howard, Irene W. Wanjala, Truc Chi T. Pham, Abby L. Parrill, Daniel L. Baker *

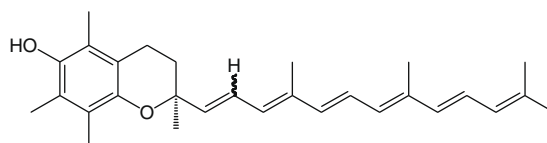


Pipemidic acid analogs were the most potent among our previously identified non-lipid small molecule inhibitors of the anticancer target enzyme, autotaxin.

Synthesis of α -tocohexaenol (α -T6) a fluorescent, oxidatively sensitive polyene analogue of α -tocopherol

pp 777–786

Yongsheng Wang, Candace Panagabko, Jeffrey Atkinson *

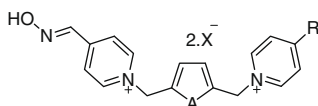


Peroxidation sensitive fluorescent Vitamin E

Bisquaternary pyridinium oximes: Comparison of in vitro reactivation potency of compounds bearing aliphatic linkers and heteroaromatic linkers for paraoxon-inhibited electric eel and recombinant human acetylcholinesterase

pp 787–794

Sandip B. Bharate, Lili Guo, Tony E. Reeves, Douglas M. Cerasoli, Charles M. Thompson *



R = CONH₂; A = S (52% reactivation and k_r 0.0417 min⁻¹ for EeAChE)

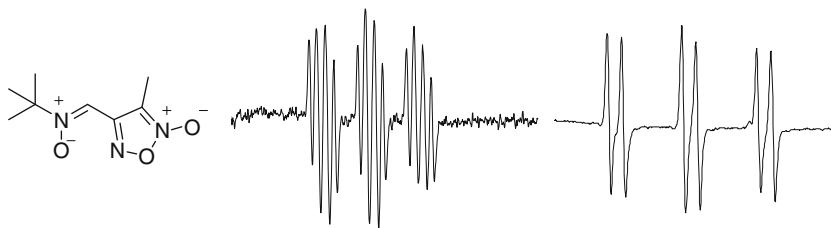
R = CHNOH; A = O (52% reactivation and k_r 0.0423 min⁻¹ for EeAChE)

A reactivation potency of new series of bisquaternary pyridinium oximes with heteroaromatic linkers (thiophene, furan, isoxazole) for paraoxon-inhibited electric eel AChE and recombinant human AChE is reported. Compounds bearing thiophene and furan linker showed comparable reactivation potency to trimedoxime and obidoxime at 10⁻⁵ M.

New heteroaryl nitrones with spin trap properties: Identification of a 4-furoxanyl derivative with excellent properties to be used in biological systems

pp 795–802

Germán Barriga, Claudio Olea-Azar^{*}, Ester Norambuena, Ana Castro, Williams Porcal^{*}, Alejandra Gerpe, Mercedes González, Hugo Cerecetto

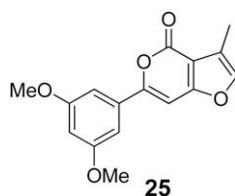


A new series of heteroaryl nitrones bearing furoxanyl and thiadiazolyl moieties were evaluated for their free radical-trapping properties.

Antitumor agents 270. Novel substituted 6-phenyl-4H-furo[3,2-c]pyran-4-one derivatives as potent and highly selective anti-breast cancer agents

pp 803–808

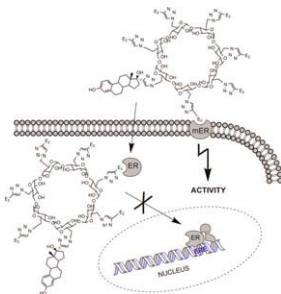
Yizhou Dong, Qian Shi^{*}, Kyoko Nakagawa-Goto, Pei-Chi Wu, Susan L. Morris-Natschke, Arnold Brossi, Kenneth F. Bastow^{*}, Jing-Yu Lang, Mien-Chie Hung, Kuo-Hsiung Lee^{*}



Click synthesis of estradiol–cyclodextrin conjugates as cell compartment selective estrogens

pp 809–821

Hye-Yeong Kim, Johann Sohn, Gihani T. Wijewickrama, Praneeth Edirisinghe, Teshome Gherezghiher, Madhubani Hemachandra, Pei-Yi Lu, R. Esala Chandrasena, Mary Ellen Molloy, Debra A. Tonetti, Gregory R. J. Thatcher^{*}

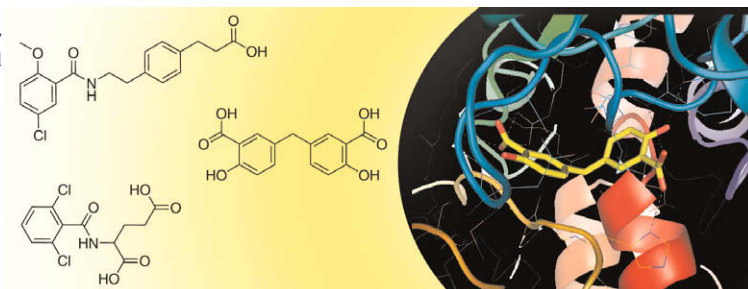


Novel and selective DNA methyltransferase inhibitors: Docking-based virtual screening and experimental evaluation

pp 822–829

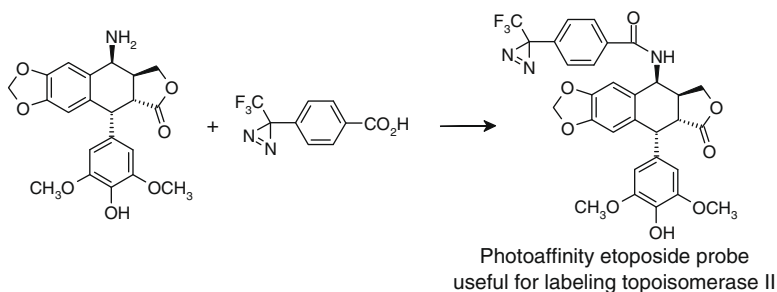
Dirk Kuck, Narendra Singh, Frank Lyko, Jose L. Medina-Franco^{*}

The first small molecules reported with biochemical selectivity towards an individual DNMT enzyme were discovered by virtual screening and experimental characterization.

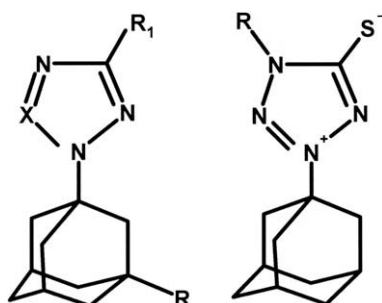


A diazirine-based photoaffinity etoposide probe for labeling topoisomerase II

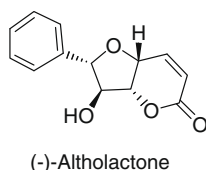
pp 830–838

Gaik-Lean Chee ^{*}, Jack C. Yalowich, Andrew Bodner, Xing Wu, Brian B. Hasinoff**Synthesis and anti-viral activity of azolo-adamantanes against influenza A virus**

pp 839–848

Vladimir V. Zarubaev ^{*}, Efim L. Golod, Pavel M. Anfimov, Anna A. Shtro, Victor V. Saraev, Alexey S. Gavrilov, Alexander V. Logvinov, Oleg I. Kiselev**Apoptotic activities in closely related styryllactone stereoisomers toward human tumor cell lines: Investigation of synergism of styryllactone-induced apoptosis with TRAIL**

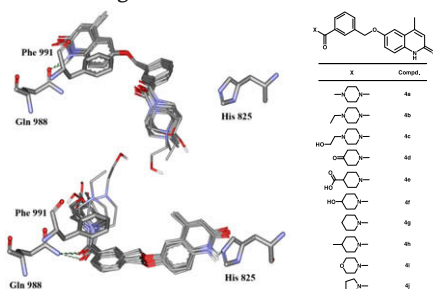
pp 849–854

Shuchi Gupta, Lee Poeppelman, Channing L. Hinman, James Bretz, Richard A. Hudson, L. M. Viranga Tillekeratne ^{*}

A comparative study of the apoptotic activities of a related group of styryllactones and the potential of one of them, (-)-altholactone, to act synergistically with TRAIL (tumor necrosis factor-related apoptosis-inducing ligand) are discussed.

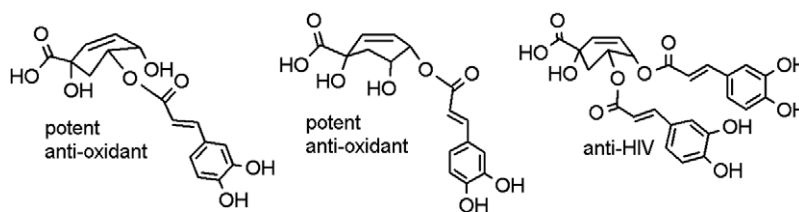
Design, synthesis and biological evaluation of 6-(benzyloxy)-4-methylquinolin-2(1H)-one derivatives as PDE3 inhibitors

pp 855–862

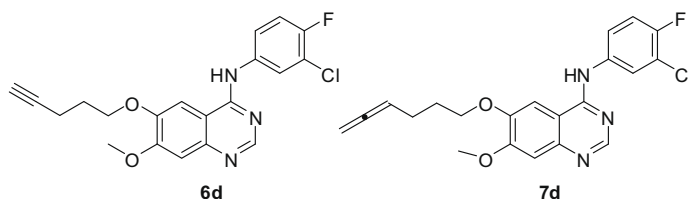
Mohsen Nikpour, Hamid Sadeghian ^{*}, Mohammad Reza Saberi, Reza Shafiee Nick, Seyed Mohammad Seyedi, Azar Hosseini, Heydar Parsaee, Alireza Taghian Dasht Bozorg

Synthesis, anti-HIV and anti-oxidant activities of caffeoyl 5,6-anhydroquinic acid derivatives

pp 863–869

Chao-Mei Ma, Takuya Kawahata, Masao Hattori^{*}, Toru Otake, Lili Wang, Mohsen Daneshmand**Enhancement of EGFR tyrosine kinase inhibition by C–C multiple bonds-containing anilinoquinazolines**

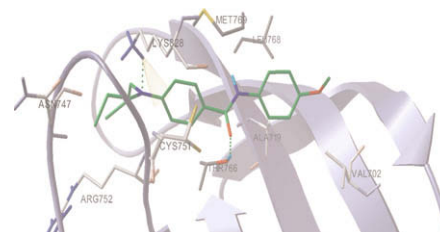
pp 870–879

Hyun Seung Ban, Yuko Tanaka, Wataru Nabeyama, Masako Hatori, Hiroyuki Nakamura^{*}**Synthesis, biological evaluation and molecular docking studies of amide-coupled benzoic nitrogen mustard derivatives as potential antitumor agents**

pp 880–886

Qing-Zhong Zheng, Fei Zhang, Kui Cheng, Ying Yang, Yu Chen, Yong Qian, Hong-Juan Zhang, Huan-Qiu Li, Chang-Fang Zhou, Shu-Qing An^{*}, Qing-Cai Jiao^{*}, Hai-Liang Zhu^{*}

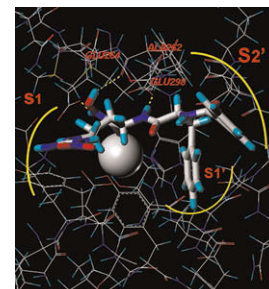
Of all the studied compounds, compounds **5b** and **5t** exhibited the most potent EGFR and HER-2 inhibitory activity. Docking simulation was performed to position compounds **5b** and **5t** into the EGFR active site to determine the probable binding model. Antiproliferative assay results indicated that some of the benzoic nitrogen mustard derivatives possessed high antiproliferative activity against MCF-7. In particular, compounds **5b** and **5t** with potent inhibitory activity in tumor growth inhibition may function as potential antitumor agents.

**Design, synthesis and primary activity assay of bi- or tri-peptide analogues with the scaffold L-arginine as amino-peptidase N/CD13 inhibitors**

pp 887–895

Jiajia Mou, Hao Fang, Yingzi Liu, Luqing Shang, Qiang Wang, Lei Zhang, Wenfang Xu^{*}

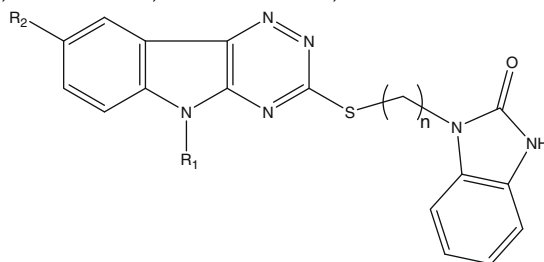
A series of bi- or tri-peptide analogues with the scaffold L-arginine were designed, synthesized and evaluated for their inhibitory activities against APN and metalloproteinase-2 (MMP-2). All of the compounds exhibited higher selectivity. Within this series, compound **C6** and **C7** (IC_{50} = 4.2 and 4.3 μ M) showed comparable APN inhibitory activities with the positive control bestatin (IC_{50} = 3.8 μ M).



Identification of triazinoindol-benzimidazolones as nanomolar inhibitors of the *Mycobacterium tuberculosis* enzyme TDP-6-deoxy-D-xylo-4-hexopyranosid-4-ulose 3,5-epimerase (RmlC)

pp 896–908

Sharmila Sivendran, Victoria Jones, Dianqing Sun, Yi Wang, Anna E. Grzegorzewicz, Michael S. Scherman, Andrew D. Napper, J. Andrew McCammon, Richard E. Lee, Scott L. Diamond, Michael McNeil *

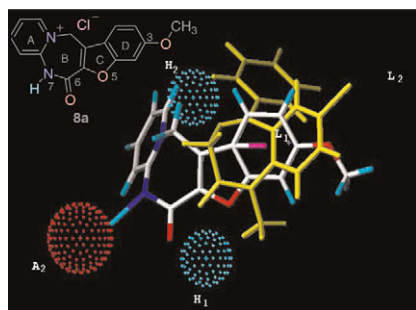


A series of triazinoindol-benzimidazolones have been shown to inhibit TDP-6-deoxy-D-xylo-4-hexopyranosid-4-ulose 3,5-epimerase (RmlC).

Synthesis, pharmacological studies and molecular modeling of some tetracyclic 1,3-diazepinium chlorides

pp 909–921

Julie-Ann A. Grant, Tamicka Bonnick, Maxine Gossell-Williams, Terry Clayton, James M. Cook, Yvette A. Jackson *

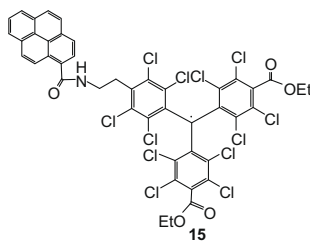


Some 1,3-diazepinium chlorides were examined for their effect on the central nervous system, and their activity compared to that of diazepam.

Perchlorotriptyl radical-fluorophore conjugates as dual fluorescence and EPR probes for superoxide radical anion

pp 922–929

Jinhua Wang, Vinh Dang, Wei Zhao, Dongning Lu, Brian K. Rivera, Frederick A. Villamena, Peng George Wang, Periannan Kuppusamy *

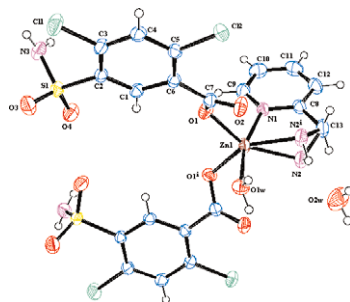


Perchlorotriptyl radicals conjugated with a fluorophore were synthesized and characterized for reaction with superoxide and detection by EPR spectroscopy and fluorescence.

Synthesis, characterization and antiglaucoma activity of a novel proton transfer compound and a mixed-ligand Zn(II) complex

pp 930–938

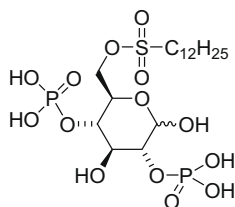
Cengiz Yenikaya *, Musa Sarı, Metin Bülbül, Halil İlkimen, Hülya Çelik, Orhan Büyükgüngör



Development of carbohydrate-derived inhibitors of acid sphingomyelinase

pp 939–944

Anke G. Roth, S. Redmer, Christoph Arenz *

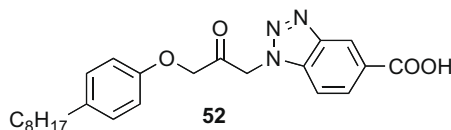


A carbohydrate-derived analogue of potent and selective acid sphingomyelinase inhibitor phosphatidylinositol-3,5-bisphosphate was synthesized. This compound is more potent and as selective as its parent compound.

**1-Indol-1-yl-propan-2-ones and related heterocyclic compounds as dual inhibitors of cytosolic phospholipase A₂ and fatty acid amide hydrolase**

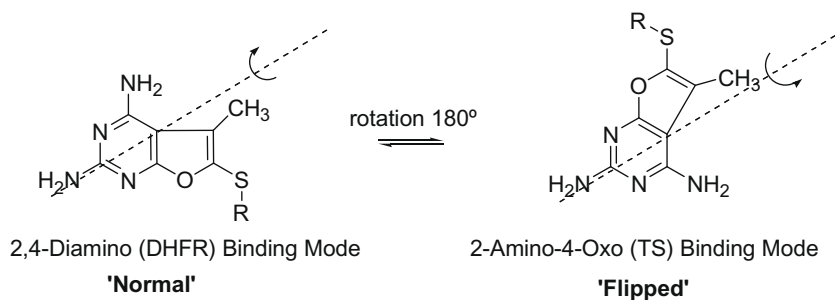
pp 945–952

Laura Forster, Joachim Ludwig, Martina Kaptur, Stefanie Bovens, Alwine Schulze Elfringhoff, Angela Holtfrerich, Matthias Lehr *

**2,4-Diamino-5-methyl-6-substituted arylthio-furo[2,3-d]pyrimidines as novel classical and nonclassical antifolates as potential dual thymidylate synthase and dihydrofolate reductase inhibitors**

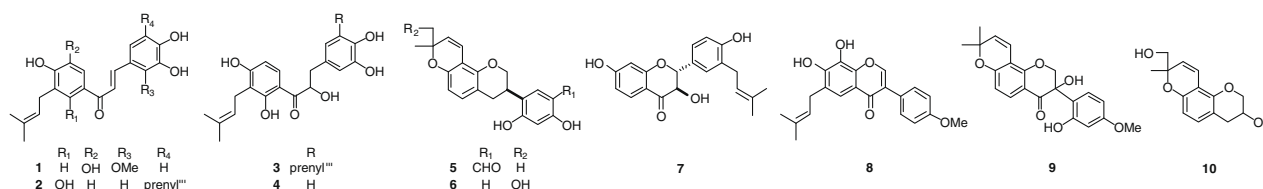
pp 953–961

Aleem Gangjee *, Hiteshkumar D. Jain, Jaclyn Phan, Xin Guo, Sherry F. Queener, Roy L. Kisliuk

**Phenolics from *Glycyrrhiza glabra* roots and their PPAR- γ ligand-binding activity**

pp 962–970

Minpei Kuroda *, Yoshihiro Mimaki *, Shinichi Honda, Hozumi Tanaka, Shinichi Yokota, Tatsumasa Mae

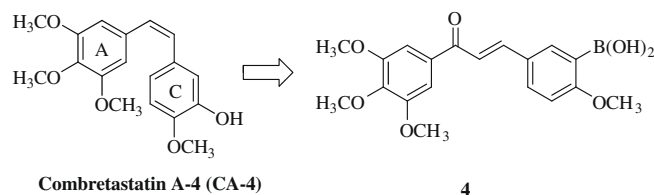


Bioassay-guided fractionation of the EtOH extract of licorice (*Glycyrrhiza glabra* roots), using a GAL-4-PPAR- γ chimera assay method, resulted in the isolation of 39 phenolics, including 10 new compounds (1–10).

A boronic acid chalcone analog of combretastatin A-4 as a potent anti-proliferation agent

pp 971–977

Yali Kong, Kan Wang, Michael C. Edler, Ernest Hamel, Susan L. Mooberry, Mikell A. Paige, Milton L. Brown *



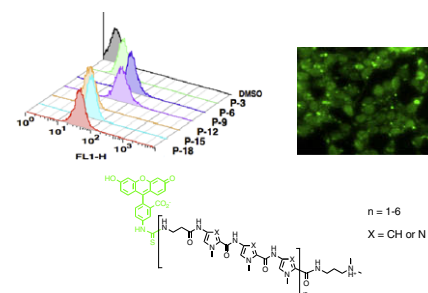
Boronic acid chalcone analogs of combretastatin A-4 were designed and synthesized. The cytotoxicity study identified that the boronic acid chalcone **4** was potent towards 16 human cancer cell lines with GI_{50} values in the range of 10–200 nM, and another three cell lines with GI_{50} values below 10 nM.

Cell permeability of Py-Im-polyamide-fluorescein conjugates: Influence of molecular size and Py/Im content

pp 978–983

Shigeki Nishijima, Ken-ichi Shinohara, Toshikazu Bando *, Masafumi Minoshima, Gengo Kashiwazaki, Hiroshi Sugiyama *

In order to investigate the influence of molecular size and pyrrole (Py)/imidazole (Im) content on the cell permeability of Py-Im-polyamide-fluorescein conjugates we systematically designed the Py-polyamides and Im-polyamides. Flow cytometric analysis revealed that Py-polyamides, even those with large molecular size, **P-15** and **P-18**, showed good cellular uptake, but Im-polyamides showed very poor uptake. Fluorescence microscopy revealed that conjugate **P-6** exhibited nuclear localization, while **P-18** showed less nuclear stain but intracellular localization, suggesting that increased molecular size is one of the determinants in reducing nuclear access. Furthermore, results for hairpin polyamide conjugates **H-1**, **H-2**, and **H-3** containing different Py/Im content indicated that cellular uptake increases as the Im residue is reduced. It appears that Py-Im-polyamide has general properties regardless of whether they have a linear or a hairpin structure.



OTHER CONTENTS

Corrigenda

pp 984–986

*Corresponding author

i+ Supplementary data available via ScienceDirect

COVER

An insight into biologically relevant chemical space showing the scaffolds of potential natural-product based inhibitors orbiting their target, the protein structure of protein 11-beta steroid dehydrogenase (PDB code 1xu7). Graphic produced using Pymol (<http://www.pymol.org>). [M. A. Koch, A. Schuffenhauer, M. Scheck, S. Wetzel, M. Casaulta, A. Odermatt, P. Ertl, H. Waldmann, Charting biologically relevant chemical space: A structural classification of natural products (SCONP), *PNAS* **2005**, 102, 17272–17277 and S. Wetzel, H. Waldmann, Cheminformatic analysis of natural products and their chemical space, *Chimia* **2007**, 61(6), 355–360].

Indexed/Abstracted in: Beilstein, Biochemistry & Biophysics Citation Index, CANCERLIT, Chemical Abstracts, Chemistry Citation Index, Current Awareness in Biological Sciences/BIOBASE, Current Contents: Life Sciences, EMBASE/Excerpta Medica, MEDLINE, PASCAL, Research Alert, Science Citation Index, SciSearch, TOXFILE. Also covered in the abstract and citation database SCOPUS®. Full text available on ScienceDirect®



ELSEVIER

ISSN 0968-0896